

# Robust $H_\infty$ Control Design for Belt-Drive with Dead-Zone Model including Viscous Coupling

M2016SC014 Yuto OTA

Isao TAKAMI

## Abstract

This paper presents the exact backlash angle function by adding “viscous coupling”, the robust stability compensation for the variation parameter, and positioning control system by  $H_\infty$  control theory. First, the control target is represented by the mathematical model with dead-zone model. Second, The viscous coupling is identified with damping ratio method. Third, the variation of the system is represented by polytope. Fourth, the robust  $H_\infty$  controller is designed for belt-drive system with the backlash and parameter variation. Finally, the robust  $H_\infty$  controller is verified by conducting simulations.

## 1 INTRODUCTION

The power train means the mechanical device which conveys rotary power by using belt. It is applied in many sectors of industry, for example, the timing belt of car engine(Continuously Variable Transmission, CVT), the belt conveyor of factory and so on. The advantages of this belt-drive system are to decrease noise and to improve transmission efficiency. The disadvantage of this system is existence of a small gap between a pair of mating gears and belt. Positioning performance degradation is caused by this gap. This small gap is called “backlash”. There exist many models of the backlash compensation. In basic control literature, dead-zone model for control design is often used[2][3]. Those studies are viewed that transmitted torque by the effect of backlash is tension of belt. However, according to [1], the rubber have internal damping as feature. this characteristic of material is known as viscous coupling(internal damping). Thus we considered similarly viscous coupling as transmitted torque, and aimed to obtain exact backlash angle function. Furthermore, viscous coupling and tension of belt are considered as transmitted torque, backlash is expressed by dead-zone model, and the backlash angle function is derived using this model. Finally the control design is completed by considering the backlash angle function as the disturbance. Here, the belt-drive experimental device used in this study is shown in Fig.1.

This experimental device includes two disks(drive and load disks), and can be put the weight on them. In addition, it is possible to change the value of backlash.



Fig 1 belt-drive experimental device

## 2 MODERING

### 2.1 Control Target

A schematic diagram of the experimental device is shown in Fig 2. Furthermore Table 1 shows physical constants and variables used in this study.

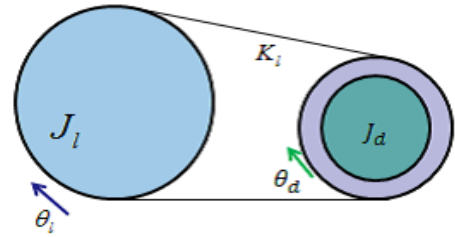


Fig 2 schematic diagram

Table 1 physical constants and variables

character	detail	unit
$\theta_d$	Drive Disc angle	[rad]
$\theta_l$	Load Disc angle	[rad]
$J_d$	Inertia of Drive Disc	[kgm <sup>2</sup> ]
$J_l$	Inertia of Load Disc	[kgm <sup>2</sup> ]
$\tau$	Motor torque	[Nm]
$K_l$	The Belt Elasticity	[Nm/rad]
$c_d$	Viscous Motor Friction	[Nm/rad/s]
$c_l$	Viscous Load Friction	[Nm/rad/s]
$T_s$	Two transmitted torque	[Nm]

### 2.2 Drive and Load disks Dynamics

Drive and Load disks Dynamics are derived by using Newton’s motion equation as Eq.(1),(2).

$$J_d \ddot{\theta}_d(t) = -c_d \dot{\theta}_d(t) + T_s(t) \quad (1)$$

$$J_l \ddot{\theta}_l(t) = -c_l \dot{\theta}_l(t) - T_s(t) + \tau(t) \quad (2)$$

According to [2],[3], Transmitted torque  $T(t)$  is shown as follows.

$$T(t) = K_l(\theta_d(t) - \theta_l(t) + \theta_{backlash}(t)) \quad (3)$$

However, the rubber have internal damping as feature, which this characteristic of material is known as viscous coupling(internal damping). Therefore, two transmitted torque can be expressed as Eq.(4).

$$\begin{aligned} T_s(t) &= K_l(\theta_d - \theta_l + \theta_{backlash}) + \sigma(\dot{\theta}_d - \dot{\theta}_l + \dot{\theta}_{backlash}) \\ &= K_l \left\{ \theta_d - \theta_l + \theta_{backlash} + \frac{\sigma}{K_l}(\dot{\theta}_d - \dot{\theta}_l + \dot{\theta}_{backlash}) \right\} \end{aligned} \quad (4)$$

Here,  $\theta_{backlash}(t)[rad]$ ,  $\sigma[Nm/rad/s]$  are the backlash angle function and the viscous coupling coefficient.

### 2.3 Dead-zone model

First, the backlash model is defined as the situation illustrated in Fig 3[2].

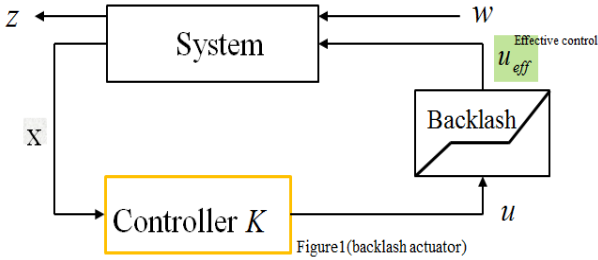


Fig 3 Backlash model

Here,  $x$ ,  $u$ ,  $u_{eff}$ ,  $z$ ,  $w$  are the state values, the control input, the effective control, the cost output, and the disturbance. The backlash nonlinearity is captured here using dead zone model. Here, define the case with  $\theta_{backlash} = -\alpha$  and  $\dot{\theta}_{backlash} = 0$  as Left contact and the case with  $\theta_{backlash} = \alpha$  and  $\dot{\theta}_{backlash} = 0$  as Right contact. We say that there is contact if there is either Left contact or Right contact. In case of Left contact,  $T_s$  is expresses as Eq.(5).

$$T_s(t) = K_l(\theta_d(t) - \theta_l(t) - \alpha) + \sigma(\dot{\theta}_d(t) - \dot{\theta}_l(t) + 0) > 0 \quad (5)$$

In case of Right contact,  $T_s$  is expressed as Eq.(6).

$$T_s(t) = K_l(\theta_d(t) - \theta_l(t) + \alpha) + \sigma(\dot{\theta}_d(t) - \dot{\theta}_l(t) + 0) < 0 \quad (6)$$

In case of Non contact,  $T_s$  is expressed as Eq.(7)

$$T_s(t) = 0 \quad (7)$$

Therefore dead-zone function is represented by Eq.(8).

$$D_\alpha(t) = \begin{cases} E - \alpha, & E > \alpha \\ 0, & |E| \leq \alpha \\ E + \alpha, & E < -\alpha \end{cases} \quad (8)$$

$$E = \theta_d(t) - \theta_l(t) + \frac{\sigma}{K_l}(\dot{\theta}_d(t) - \dot{\theta}_l(t)) \quad (9)$$

Where,  $\alpha[rad]$  is backlash angle. Eq.(8) can be rewritten as Eq.(10).

$$D_\alpha(t) = \theta_d(t) - \theta_l(t) + \frac{\sigma}{K_l}(\dot{\theta}_d(t) - \dot{\theta}_l(t)) + \theta_{backlash}(t) \quad (10)$$

From Eq.(8)-(10),  $\theta_{backlash}(t)$  is described as Eq.(11).

$$\theta_{backlash}(t) = \begin{cases} -\alpha, & E > \alpha \\ -E, & |E| \leq \alpha \\ \alpha, & E < -\alpha \end{cases} \quad (11)$$

### 2.4 State Space Representation

Let state variable  $x(t)$ , input  $u(t)$ , and disturbance  $w(t)$  be Eq.(12),(13),and (14).

$$x(t) = \begin{bmatrix} \theta_d(t) & \dot{\theta}_d(t) & \theta_l(t) & \dot{\theta}_l(t) \end{bmatrix}^T \quad (12)$$

$$u(t) = \tau(t) \quad (13)$$

$$w(t) = \theta_{backlash}(t) \quad (14)$$

From Eq.(1),(2),(4), and (11)-(14), the state-space representation of belt-drive system is derived as Eq.(15).

$$\begin{cases} \dot{x}(t) = Ax(t) + B_1w(t) + B_2u(t) \\ y(t) = Cx(t) \end{cases} \quad (15)$$

$$A = \begin{bmatrix} 0 & 1 & 0 & 0 \\ -\frac{K_l}{J_d} & \frac{c_d+\sigma}{J_d} & \frac{K_l}{J_d} & \frac{c_d}{J_d} \\ 0 & 0 & 0 & 1 \\ \frac{K_l}{J_l} & \frac{\sigma}{J_l} & -\frac{K_l}{J_l} & -\frac{c_d+\sigma}{J_l} \end{bmatrix}$$

$$B_1 = \begin{bmatrix} -\frac{K_l}{J_d} \\ 0 \\ 0 \\ \frac{K_l}{J_l} \end{bmatrix}, B_2 = \begin{bmatrix} 0 \\ \frac{1}{J_d} \\ 0 \\ 0 \end{bmatrix}, C = \begin{bmatrix} 0 & 0 & 1 & 0 \end{bmatrix}$$

### 2.5 Servo System

In this study, the servo system is used for removed the steady-error. Let  $e(t)[rad]$  be the error between the measurable out put  $y(t)$  and the reference  $r(t)[rad]$ . The state variable for the servo system is expressed as Eq.(16).

$$x_e = \begin{bmatrix} x(t) & \int e(t) \end{bmatrix}^T \quad (16)$$

The servo system can be expressed as follows.

$$\begin{cases} \dot{x}_e(t) = A_e x_e(t) + B_{1e} w_e(t) + B_{2e} u(t) \\ y(t) = C_{1e} x_e(t) \end{cases} \quad (17)$$

$$A_e = \begin{bmatrix} A & O \\ -C & O \end{bmatrix}, B_{1e} = \begin{bmatrix} B_1 & O \\ -C & 1 \end{bmatrix}, B_{2e} = \begin{bmatrix} B_2 \\ O \end{bmatrix}$$

$$C_{1e} = \begin{bmatrix} 0 & 0 & 1 & 0 & 0 \end{bmatrix}, w_e(t) = \begin{bmatrix} \theta_{backlash}(t) \\ r(t) \end{bmatrix}$$

### 3 PARAMETER IDENTIFICATION

In this section, let us identify the viscous coupling coefficients  $\sigma$ . The damping ratio method for identifying the parameter  $\sigma$  is used. Since viscous coupling is generated by expansion and contraction of the belt, this parameter is identified by the technique as follows.

First, the Drive disk is not to be easily moved by holding the hand. Second, the Load disk is applied the force to direction of rotation by the hand. Then, the Load disk is released one's hand. Finally we observe the reference of the Load disc. The result of experiment is shown in Fig 4.

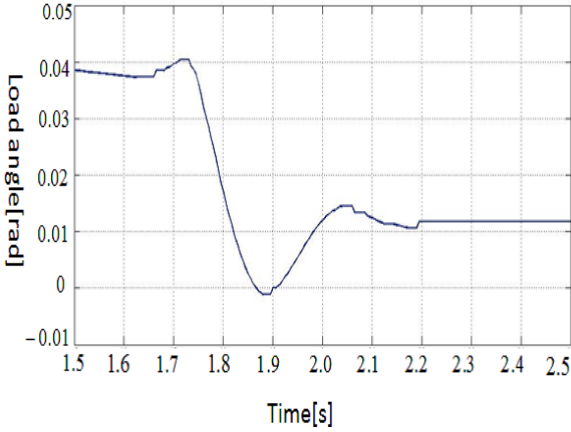


Fig 4 The reference of Load disk

The natural frequency  $\omega_n$ [Hz], damping coefficient  $\zeta$  are derived as follows.

$$\omega_n = \sqrt{\frac{K_l}{J_l}} \quad (18)$$

$$\zeta = \frac{1}{2\pi} \log_{10} \frac{X_0}{X_1} \quad (19)$$

Here,  $X_0$ ,  $X_1$  are the initial amplitude and the first amplitude. From Eq.(18) and Eq.(19), all viscous  $c$ [Nm/rad/s] given the Load disk is expressed as the following equation.

$$c = 2J_l\omega_n \times \zeta \quad (20)$$

Therefore, the viscous coupling coefficient is given as follows.

$$\sigma = c - c_l \simeq 0.0171 \quad (21)$$

### 4 CONTROL DESIGN

In this section, the controller which the robust stability for the system against variation of the inertias  $J_d$  and  $J_l$  is designed. the robust stability can be guaranteed theoretically by solving linear matrix inequality (LMI) conditions with polytopic representation.

#### 4.1 Polytopic Representation

The ranges of the variation parameters  $J_d$  and  $J_l$  is represented as following equation.

$$J_d \in [J_{d,min}, J_{d,max}] = [4.2 * 10^{-4}, 5.5 * 10^{-3}] \quad (22)$$

$$J_l \in [J_{l,min}, J_{l,max}] = [8.3 * 10^{-3}, 2.8 * 10^{-2}] \quad (23)$$

Then, the combinations of fluctuation are shown as follows.

$$\{J_{d,min}, J_{l,min}\}, \{J_{d,max}, J_{l,max}\}, \\ \{J_{d,max}, J_{l,min}\}, \{J_{d,min}, J_{l,max}\}$$

By using polytopic representation, the end points of the variation range of matrices  $A_{ei}$ ,  $B_{1ei}$ ,  $B_{2ei}$  are shown as follows.

$$A_{ei}(i = 1, 2, 3, 4), B_{1ei}(i = 1, 2, 3, 4), B_{2ei}(i = 1, 2, 3, 4)$$

#### 4.2 $H_\infty$ Control

From Eq.(15), the general plant is derived as follows.

$$\begin{cases} \dot{x}_e(t) = A_e x_e(t) + B_{1e} w_e(t) + B_{2e} u(t) \\ y(t) = C_2 x_e(t) + D_2 u(t) \end{cases} \quad (24)$$

$$C_2 = \begin{bmatrix} W_x & 0 \\ 0 & W_e \\ 0 & 0 \end{bmatrix}, D_2 = \begin{bmatrix} 0 \\ 0 \\ W_u \end{bmatrix}$$

Here,  $W_x \succ 0$ ,  $W_e \succ 0$ ,  $W_u \succ 0$  are weight matrices for the state variable, integration of error and input. Let us consider to minimize  $H_\infty$  norm from disturbance  $w_e(t)$  to the cost output  $z(t)$ .  $H_\infty$  norm is defined as follows.

$$\|G_{zw}(s)\| = \sup \frac{\|z(t)\|_2}{\|w_e(t)\|_2} \quad (25)$$

If these exist  $\|G_{zw}(s)\| \prec \gamma_\infty$ , the system is stabilized.

#### 4.3 LMI Condition

The LMI condition to derive the  $H_\infty$  controller stabilizing the system are given as follows.

**Theorem:** If these exist matrices  $X$  and  $Y$  satisfying the following LMI conditions, the system is stabilized by  $u(t) = KX_e(t) = YX^{-1}x_e(t)$ .

minimize :  $\gamma$   
subject to  $X \succ 0$

$$\begin{bmatrix} XA_{ei}^T + A_{ei}X + Y^T B_{2ei} + B_{2ei}Y & XC_2^T + Y^T D_2^T & B_{1ei} \\ C_2 + D_2 Y & -\gamma_\infty I & 0 \\ B_{1ei}^T & 0 & -\gamma_\infty I \end{bmatrix} \prec 0 \quad (i = 1, 2, 3, 4) \quad (26)$$

## 5 SIMULATION

In this section, the effectiveness of the proposed method is illustrated by simulations. In this study, the backlash angle parameter  $\alpha[rad]$  is set as  $0.1[rad]$ . Additionally, the reference of the Load disk angle  $\theta_l$  is  $\frac{\pi}{2}[rad]$ , and given by the step input. The simulation results are shown in Fig 5-8.

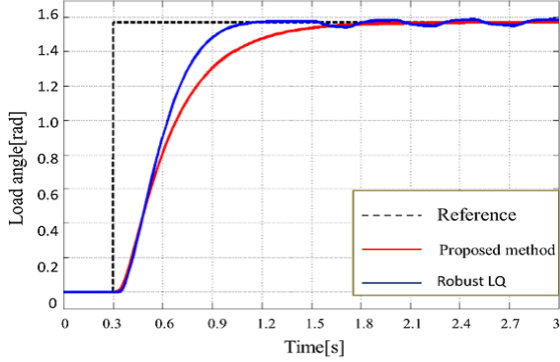


Fig 5  $J_{d,min}, J_{l,min}$

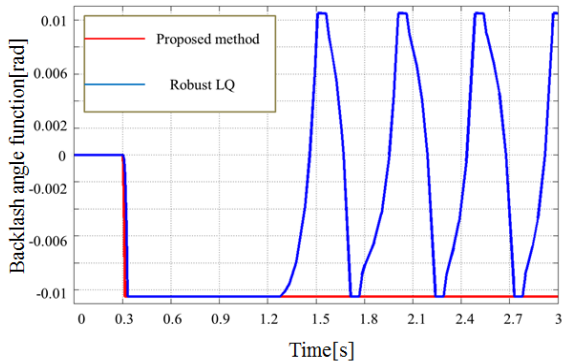


Fig 6 Disturbance  $\theta_{backlash}$

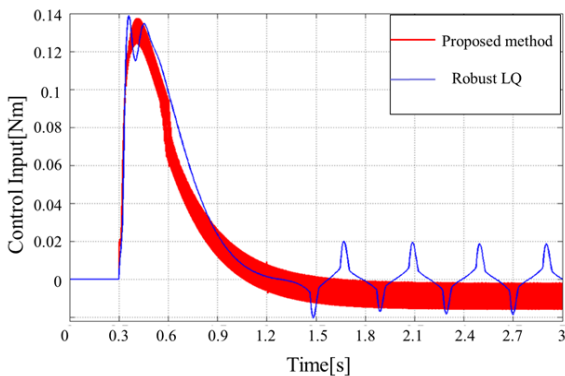


Fig 7 Input( $J_{d,min}, J_{l,min}$ )

Here, the solid line, the red line, the blue line shows the reference, the result when Load disc angle is controlled by the  $H_\infty$  controller, and the result when Load disc angle is controlled by the robust LQ controller

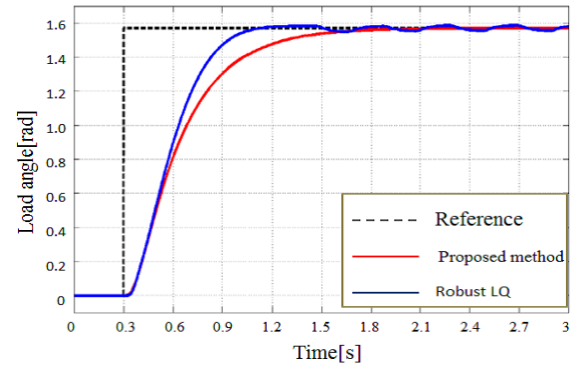


Fig 8  $J_{d,max}, J_{l,max}$

that the backlash are not guaranteed. As can be seen in Fig.5-8, the Load Disc angle follows the reference with the proposed method, and Robust  $H_\infty$  controller suppresses the vibration(the limit cycle) caused by the backlash than Robust LQ controller. Additionally, even though the system has parameter variation, the disc stably follows the reference.

## 6 CONCLUSION

In this paper, the viscous coupling is considered as the transmitted torque, obtained the exact backlash angle function by using the dead-zone model, and the robust  $H_\infty$  controller is designed for belt-drive with the backlash and parameter variation. The robust stability in the prescribed variation range of the inertia of load and drive disk is guaranteed theoretically by using polytopic representation. The backlash considered as the disturbance is guaranteed by using  $H_\infty$  control, and the problem is formulated as solving a finite set of linear matrix inequality (LMI). The effectiveness of the proposed method is illustrated by simulation by comparing with the robust LQ controller that the backlash are not guaranteed. The proposed method suppresses the vibration of the Load disk by the backlash than the robust LQ controller.

## References

- [1] M. Minowa, N. Kato and K. Onodera, "Development of Low Elastic Modulus and High Damping Rubber for Vibration Control Device", *The Japan Society of Mechanical Engineers*, Vol.52, No1, pp.39-43, May 10 (2002).
- [2] L. Acho, F. Ikhouane, G. Pujo, "Robust Control Design for Mechanisms with Backlash", *Journal of control Engineering and Technology*, Vol.3, Iss. 4, pp.175-180.October (2013).
- [3] Nordin, P.O. Gutman, "Controlling mechanical systems with backlash: A survey", *Automatica*, Vol. 38, pp. 1633-1649(2002).